Revealing The Unseen Mud Diapir Through OBN Data: A Case Study in Yinggehai Basin

J. Cai[1], Y. Liu[1], R. Tan[1], P. Deng[1], M. Wang[1], Y. Xie[1], B. Hung[1], M. Ouyang[2], D. Deng[2]

[1] CGG; [2] CNOOC

Summary

Yinggehai basin is one of the most important basins of the South China Sea for its mega gas reservoirs and exploration potential. Vintage seismic data generally suffers severely from complex structures, including diapir formed by thermal fluids, strong shallow gas fields, and complex faulting systems. The diapiric structures in particular, commonly present in the region, and have long been an 'unseen Elephant', causing much uncertainty in geological interpretation. Reprocessing vintage streamer data has not been sufficient to overcome these imaging challenges so a new OBN dataset was acquired, and the latest processing technologies applied, including visco-acoustic Time-lag FWI (TLFWI), Dynamic Resolution TLFWI (DR-TLFWI), and Diffraction Imaging. With the combined uplifts, the diapir structure is much better imaged, significantly impacting the geological interpretation within this basin.

Revealing The Unseen Mud Diapir Through OBN Data: A Case Study in Yinggehai Basin

Introduction

Yinggehai basin in the South China Sea has many diapir structures with their associated traps forming important exploration targets. Dongfang field is one of the largest gas-producing fields with estimated gas reserves of 200 billion cubic meters in the shallow. The field is rich in shallow gas pockets and channels charged by the gas from the deep source rock in the diapir structure with the faults as its migration path. Based on experience from adjacent blocks, potential reserves are also expected inside the central, deeper section of the diapir structure. However, geological interpretation inside the diapir has long been challenging due to the complex shallow overburden with poor illumination, severe kinematics distortion, attenuation, and scattering effects (Deng et al., 2020). All those characteristics lead to a severe image washout at the diapir zone as indicated by the yellow dash line in Figure 1a. Several iterations of seismic re-processing of vintage streamer data were conducted aiming for better geological understanding. However, the imaging quality was still sub-optimal leading to continued uncertainties in the diapir's internal structure. It was concluded that the vintage streamer data was insufficient for exploration purposes. Thus, to solve the diapir imaging challenge, a modern Ocean Bottom Node (OBN) acquisition was carried out in 2021 with maximum offsets beyond 16 km.

To unlock the full potential of the OBN data and address the geophysical challenges, the OBN data was run through a comprehensive processing workflow including the latest model building technology, visco-acoustic Time-lag FWI (TLFWI) (Wang et al., 2018) and Dynamic Resolution TLFWI (DR-TLFWI) (Wang et al., personal communication, 2023). Visco-acoustic TLFWI was used to jointly invert the shallow velocity as well as the quality factor (Q) body. However, due to the high-velocity layers at around 1.5 – 2.2 km depth, the diving wave penetration depth was limited to around 2.2 km, above the diapir structure. DR-TLFWI was subsequently applied to better utilize the reflection energy and invert the velocity in the diapir section. Diffraction Imaging (Lowney et al., 2020) was further employed to give clearer deep fault orientation information to aid interpretation work. The workflow gave a robust velocity model update from the shallow to deep section, addressing several issues encountered in previous processing. The improved velocity model and better illumination from the new OBN data resulted in superior images in the survey area. In this paper, we will discuss the key technologies that were used to derive a better velocity model and improve the final image quality, particularly in the interior of the diapir structure.

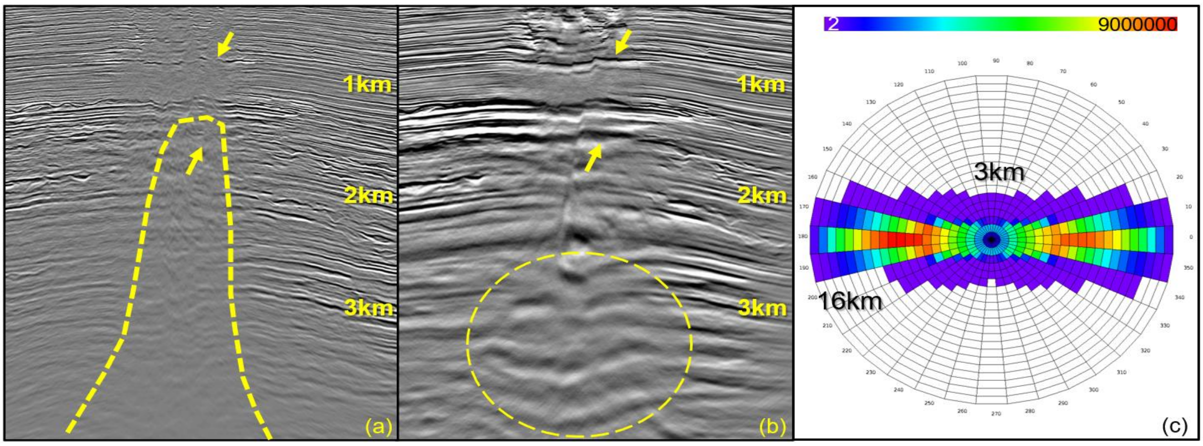

***Figure 1**: (a) vintage streamer PSDM stack with obvious washout in the diapir region as indicated by the yellow dash line; (b) new OBN PSDM stack using vintage streamer velocity with structural sagging as the yellow dash circle indicates; (c) rose diagram of the OBN acquisition.*

The Dongfang OBN data

The OBN dataset in the Dongfang field was acquired with a maximum offset X of 16 km but with a reduced maximum offset Y of 3 km due to operational constraints. Figure 1c displays the corresponding rose diagram. The receiver line and shot line direction were perpendicular to the orientation of the faults and the trapped gas body. The receiver station interval was 50 m with a receiver line interval of 200 m, whilst both shot station interval and shot line interval were 50 m. A gun volume of 4090 cu.in was used to obtain a good signal-to-noise ratio with deep penetration to the target level. A water depth of 60 – 70 meters generated receiver side ghost and peg-leg multiples with a first non-zero notch frequency at 10 – 12.5 Hz. Summation of pressure and vertical geophone components played a critical part in recovering the signals in the notch frequency ranges for the deep target zone. The rich low-frequency signal and the improved illumination from the OBN data improved the image quality (Figure 1b) even when using the smooth vintage velocity. However, there are still imaging issues due to the complexity and strong attenuation of both the shallow overburden and the diapir structure. Accurate velocity and robust Q models are essential to handle the kinematic distortion and amplitude loss. The benefits of OBN data enable the application of state-of-art technologies to address these issues. In the following sections, we will discuss these key technologies.

Velocity update at shallow gas clouds by visco-acoustic TLFWI

Gas pockets and channels in the near surface can introduce strong kinematic distortion and amplitude loss due to spatial velocity variation and absorption effects. The shallow-producing gas field covers around 200 km^2 leading to severe attenuation in any signal penetrating beneath. To compensate for the kinematic distortion and amplitude loss from this shallow overburden, both the velocity and Q models need to be accurately estimated (Wang et al., 2018). Visco-acoustic wave propagation was incorporated in TLFWI to honour the visco-acoustic effects. This allows us to jointly update the velocity and Q models, reducing crosstalk between velocity and Q in the inversion process. Figure 2a shows the PSDM stack using OBN data and vintage streamer smooth velocity. Structural sagging and amplitude dimming combined with lower resolution is observed when compared to the neighbouring area less affected by the shallow gas channels. With the updated high-resolution velocity (Figure 2b) and inverse Q model (Figure 2c) inverted by visco-acoustic TLFWI, the kinematic distortions and amplitude loss at the core of the diapir zone are well corrected in the QPSDM stack (Figure 2b). The frequency content is now more consistent with the adjacent area that suffers less from the attenuation effect. Figure 2d and 2e show the depth slices of the inverted velocity and inverse Q field at 240 m, demonstrating that the inverse Q field is high resolution and consistent with geological features.

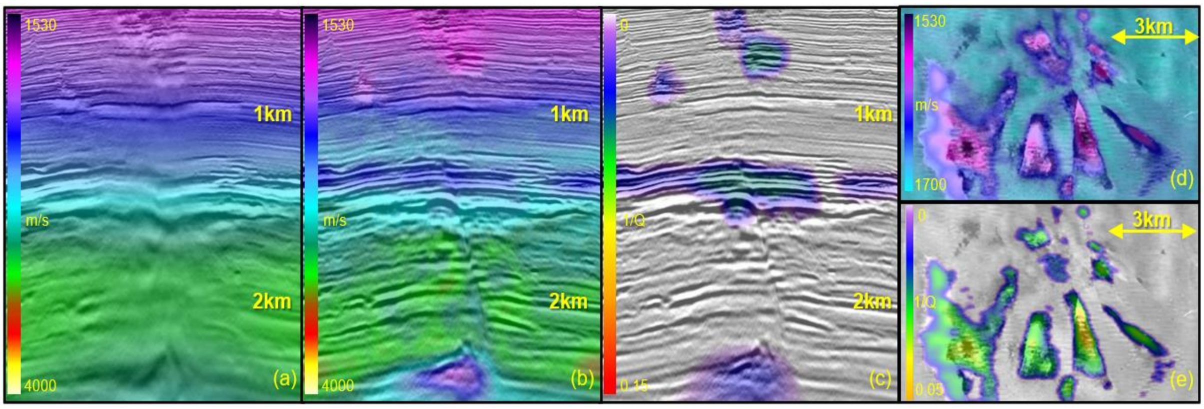

***Figure 2**: PSDM stack using vintage streamer velocity with vintage streamer velocity overlaid (a); QPSDM stack with visco-acoustic TLFWI velocity (b) and 1/Q (c) overlaid; depth slices of visco-acoustic TLFWI velocity (d) and 1/Q (e) at 240 m.*

Diapir velocity update by DR-TLFWI

The first round visco-acoustic TLFWI captures the shallow overburden velocity variations and delineates the fast velocity layer at around 1.5 – 2.2 km depth. Such high velocity, together with the extremely low velocity inside the deep diapir region, limits the penetration depth of diving waves to around 2.2 km even with the maximum offset of 16 km. In this case, the velocity update in the diapir region becomes more challenging, requiring reflections to be included. OBN data provides better reflection angle coverage than the vintage streamer data, allowing the background tomographic velocity update, based on the residual moveout information from the image gathers, to derive a much stronger velocity inversion inside the diapir structure. However, remaining high-wavenumber structural undulations are still observed, adding challenges for deep reservoir understanding and source rock analysis. A high-resolution velocity model that captures spatial variations is necessary to handle this challenge. Many studies on reflection FWI have been carried out to utilize the tomographic term for better kinematics correction (Gomes and Chazalnoel, 2017; Wang et al., 2018). Here, we use the DR-TLFWI proposed by Wang et al. (Personal communication, 2023), which extends the TLFWI framework with an additional weighting applied to the tomographic term for more effective kinematics correction with the improved horizontal model resolution from the full gradient. Figure 3a shows the PSDM stack with the velocity from TLFWI (Figure 3c) in the deep section, where the structural undulation caused by strong spatial varying velocity remains due to the deep velocity update, dominated by the migration term, having less kinematics impact. After DR-TLFWI the low-wavenumber update is more prominent in the inverted velocity model (Figure 3d), and the spatial variations from the velocity update successfully reduce the structural distortion in the PSDM stack (Figure 3b), even at depths of 5km. It is worth noting that the "stripy" looking velocity variations inside the diapir structure could be related to thermal fluid movements as well as the limited vertical resolution of the current DR-TLFWI model, which is a result of the limited reflection angle coverage in the data and limited frequency range of the inversion.

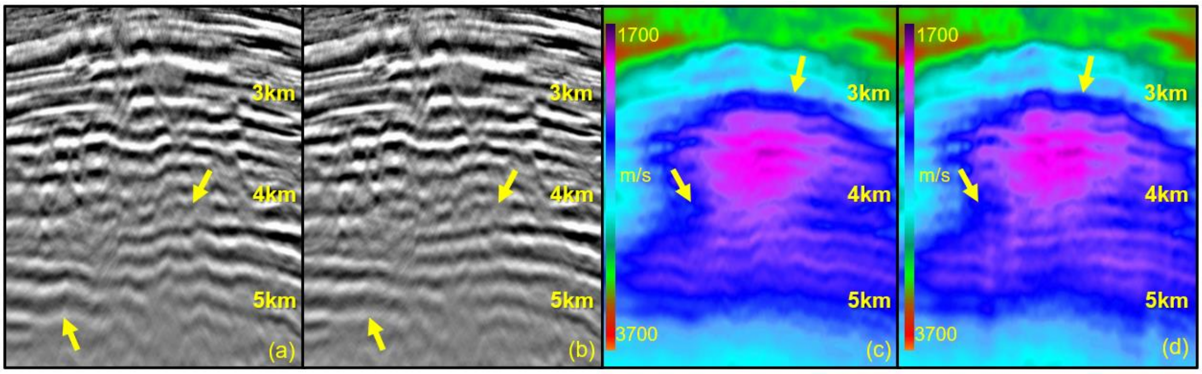

Figure 3: *PSDM stacks and the velocity models from: (a), (c) TLFWI model; (b), (d) DR-TLFWI model.*

Discussions

By combining high-quality OBN data and the latest model building techniques including visco-acoustic TLFWI and DR-TLFWI, the new OBN QPSDM provides a much-improved image of the diapir structure (Figure 4b) over the legacy streamer PSDM (Figure 4a). The faulting systems and event continuity become much clearer enabling new insight into their geological interpretation. The diapir was originally interpreted to start from 1.5 km depth beneath the mega gas field (Figure 4d) due to poor image quality from the legacy data. With the new QPSDM image, the events in the depth interval 1 – 2 km are revealed as normal gas sand reflectors. The diapir structure actually starts from 2.5 km depth and is captured by the latest velocity model as a huge velocity inversion below 3 km (Figure 4c). The significantly improved continuity of potential gas reservoirs is indicated by the red layers in Figure 4e. However, uncertainty still exists below 4 km depth, with events less coherent, and a fault system that is more difficult to track, limiting understanding of the source rock evolution. To aid the interpretations, a diffraction image was generated to better delineate the faulting distribution and orientation without contamination from reflections (Figure 4f, 4g). The uncertainty could be further mitigated by introducing wider azimuth and longer offset data, allowing diving waves to invert more reliable velocities in the deeper section. Correspondingly, this may also bring additional value to a state-of-art high-frequency FWI image (Zhang et al., 2020) as diving waves may have better illumination of the complex faulting and fractures in the deep section.

Conclusions

The diapir image of the study area was sub-optimal due to complex geology and legacy data limitation. The new image produced by the OBN data and the latest processing technologies is significantly improved which enables more accurate geological interpretation. To further reduce the image uncertainty, longer offset with wider azimuth can be considered for future acquisitions.

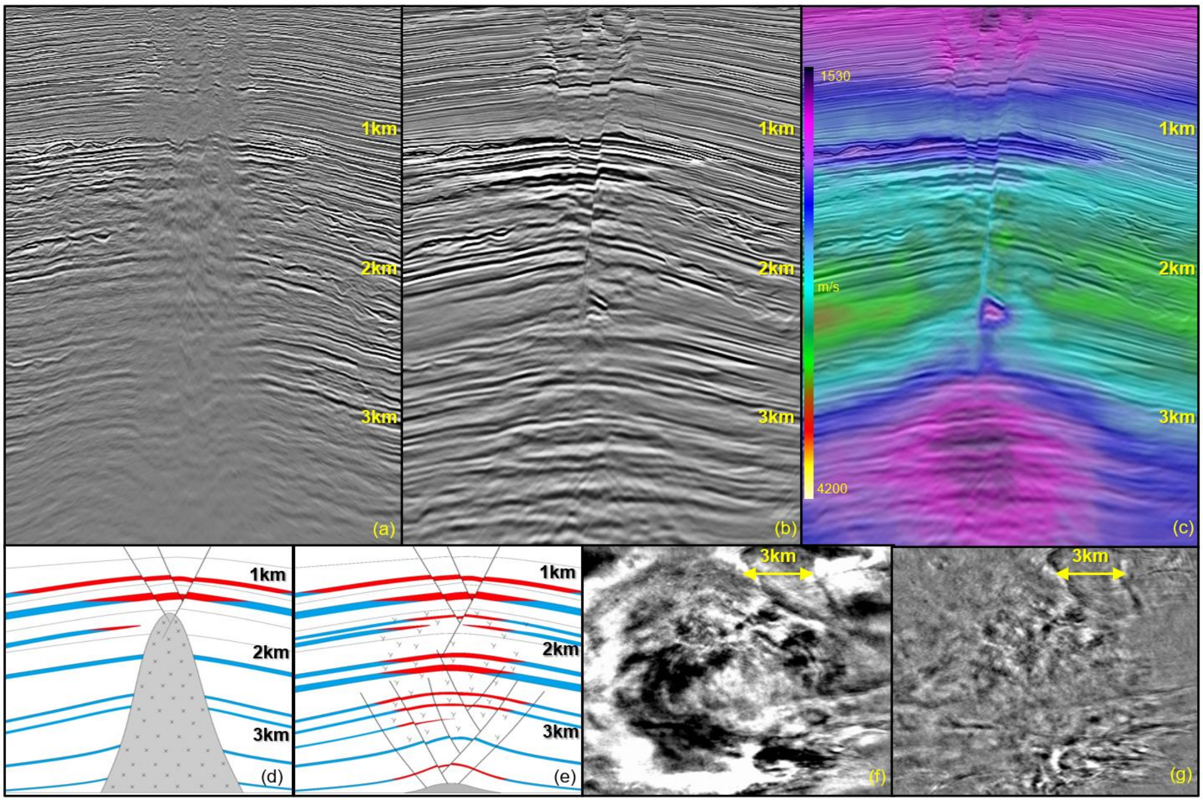

Figure 4: *Vintage streamer PSDM stack (a); OBN QPSDM stack (b) with OBN DR-TLFWI velocity overlaid (c); the geological interpretation model from vintage data (d) and OBN data (e); Depth slice of OBN QPSDM stack (f) and the corresponding diffraction image (g) at 4200 m.*

Acknowledgements

The authors thank CGG and CNOOC for permission to publish this paper. Our thanks also go to Qing Xu for the suggestions and fruitful discussions during the work.

References

Deng, Y., Pang, G., Li, H., Zhang, Y. and Ren, T. [2020]. Analysis on genesis and imaging countermeasures on the diapir fuzzy area in Yinggehai basin. *China Offshore Oil and Gas*, 32 (3):59.

Gomes, A. and Chazalnoel, N. [2017]. Extending the reach of FWI with reflection data: Potential and challenges. *87th SEG International Exposition and Annual Meeting*, Expanded Abstracts, 1454-1459.

Lowney, B., Hoeber, H., Kaszycka, E. and Hou, S. [2020]. Combined Pre- and Post-Migration Diffraction Separation. *82nd EAGE Conference & Exhibitions*, Expanded Abstracts, pp. 1-5.

Wang, M., Xie, Y., Xiao, B., Ratcliffe, A. and Latter, T. [2018]. Visco-acoustic full-waveform inversion in the presence of complex gas clouds. *88th SEG International Exposition and Annual Meeting*, Expanded Abstracts, 5516-5520.

Wang, P., Zhang, Z., Wei, Z. and Huang, R. [2018]. A demigration-based reflection full-waveform inversion workflow. *88th SEG International Exposition and Annual Meeting*, Expanded Abstracts, 1138-1142.

Zhang, Z., Wu, Z., Wei, Z., Mei, J., Huang, R. and Wang, P. [2020]. FWI Imaging: Full-wavefield imaging through full-waveform inversion. *90th SEG International Exposition and Annual Meeting*, Expanded Abstracts, 656-660.